Carbon nanotube based composite membranes for water desalination by membrane distillation

Ludovic Dumée[1,2,#], Kallista Sears[1#], Jürg Schütz[1], Niall Finn[1]

[1] *CSIRO Materials Science and Engineering, Bayview Ave, Clayton Vic 3168, Australia*

Stephen Gray[2], Mikel Duke[2]

[2] *Victoria University Werribee Campus, Hoppers Lane, Werribee PO Box 14428 Melbourne, Victoria, 8001, Australia*

Corresponding authors: # ludovic.dumee@csiro.au & kallista.sears@csiro.au

Comment [MCD1]: Stephen's name should be last as he is the project leader.

Abstract— **New technologies are required to improve desalination efficiency and increase water treatment capacities. One promising low energy technique to produce potable water from either sea or sewage water is Membrane Distillation (MD). However, to be competitive with other desalination processes, membranes need to be designed specifically for the MD process requirements. Here we report on the design of Carbon Nanotube (CNT) based composite material membranes for Direct Contact Membrane Distillation (DCMD). The membranes have been thoroughly characterized and also tested in a DCMD setup under different feed temperatures and test conditions. We demonstrate that Bucky-paper membranes can be used for purification of synthetic seawater via the DCMD process and, most importantly, that the composite Bucky-paper (BP) structures show improved lifetime and performance compared to their self-supporting BP counterparts.**

I. INTRODUCTION

Carbon nanotube (CNT) [1] based membranes have attracted interest over the past 5 years. Several groups have reported on CNT composite material membranes for applications such as pervapouration of cyclohexane/benzene [2], nanofiltration [3]-[4] and separation of hydrocarbons [5]. However to our knowledge no-one has focused on CNT based membranes for use in Membrane Distillation (MD). MD is an alternative technique for the purification of sea or sewage water. In a Direct Contact Membrane Distillation (DCMD) setup a hydrophobic membrane acts as a barrier between a warm feed (e.g. sea water) and a cold permeate of fresh water. A difference in water vapour pressure is generated due to the temperature gradient across the membrane and leads to water vapour transfer from the hot to cold side. The water vapour condenses on the cold side creating fresh water as illustrated by the schematic in Figure 1 [6]-[7]-[8]. However, specific membranes need to be designed for MD to become competitive with other desalination techniques.

We previously demonstrated that CNT Bucky-paper (BP) membranes, a non-woven structure of entangled CNTs, could be used to desalinate synthetic seawater via DCMD process[9]. However ageing of the membranes over time limited their performance.

This paper focuses on processing composite structures from the CNT BPs, as a method of improving membrane lifetime and performance. These CNT composite membranes were characterized and tested in a DCMD test apparatus.

Deleted: setup.

EXPERIMENTAL DETAILS

A. Carbon nanotube growth

The CNTs were grown by chemical vapor deposition at CSIRO Material Science and Engineering, Melbourne Australia. A 5 nm thick iron catalyst film was deposited onto a silicon substrate bearing a thin Silicon Dioxide layer. A mixture of Helium (95%) - Acetylene (5%) was used as the carbon feedstock and heated to between 650 and 750°C. The CNTs typically have an outer diameter of ~10-15 nm and length of 150-300 μm [10].

B. Carbon nanotube bucky-paper composite material membrane fabrication

First, as grown CNTs were dispersed in propan-2-ol. The suspensions were sonicated up to 5 times, for 15 minutes and at 150 W, in a sonicating bath. Once well-dispersed CNT suspensions were achieved, they were filtered through a Millipore filtration unit. The CNTs were captured on a Poly-ether-sulfone (PES) membrane (0.22 μm pore size, Millipore) to produce a self-supporting CNT BP. As shown in Figure 2, the structure morphology appears to be a randomly entangled network of fully dispersed CNTs.

Composite CNT BP membranes were produced by three methods. The first method involved hot pressing self-supporting BPs between two layers of porous poly-propylene (PP) supports (55% porosity, Figure 3). The three layers were maintained between two stainless steel plates and hot-pressed at low pressures for 15 min at 80ºC. This structure is referred to throughout the text as the "sandwiched BP" composite.

Deleted: ~55%

The second structure is a slight variation of the first and referred to as the "filtered sandwiched BP" composite. Suspensions of dispersed CNTs were filtered through a PP support (with a PES membrane underneath). In this case the CNTs are collected on and within the pores of the PP support. The PP-CNT cake was sandwiched with another layer of poly-propylene support and the layers hot-pressed together under the same conditions mentioned above.

Finally, a number of "polymer infiltrated BP" membranes were formed by partially embedding a self-supporting BPs by vacuum filtration of a polymer/solvent solution, across the self-supporting membrane. Solutions at 5% of either Poly-Styrene (PS) or Poly-Vinyl Di-Fluoride (PVDF) in Di-Methyl-Formamide (DMF) were used. After polymer infiltration, 99.99% pure DMF was filtered through the membrane to remove any non-bonded polymer.

Poly-Tetra-Fluoro-Ethylene (PTFE) 0.22 micron nominal pore size membranes, purchased from

Millipore, were also characterized and tested as control membranes.

C. Membrane characterization

Scanning electron microscopy (SEM) was used to investigate the surface structure of the composite BP membranes and was performed with a Philips FEG SEM at 2 kV and 7.5 mm working distance. An FEI Nova nanolab 200 Dual Beam Focused Ion Beam (FIB) was used to form cross sections of the BP membranes. Milling was performed with a 1 nA, 30 kV Ga ion beam, followed by 0.3 nA cleaning steps. Contact angles were measured with a 2 mL pycnometer as described in [11]. An average BET surface area was determined by N_2 adsorption on a Micromeretics Tristar 3000 [12]. The samples were first degassed for 70 hours and then analysed at 77K. Finally, a pocket goniometer PG-3 from Fibro Systems was used to determine contact angle. The tests were performed at 20ºC with 4 µL drops of deionised water [13].

Comment [.2]: Should this be porosity rather than contact angle?

Deleted: a

D. Direct contact membrane distillation setup

In our DCMD setup the membranes were placed inside a sealed PTFE module. A peristaltic pump fitted with two coupled heads was used to control both permeate and feed flow rates, which were kept constant at 300 ml/min. The temperatures of the water streams were also kept constant and no major temperature drops between the inlet and the outlet of the module were measured. The temperature was therefore considered constant over the membrane area. The electrical conductivity and temperature of the hot and cold electrolytes as well as the water level transferred to the cold side were monitored over time and data logged. Tests were performed with deionised water and synthetic seawater (35 g/L NaCl solutions at 11 mS/cm). The membrane test area was a 25.4 mm diameter disc.

Each membrane was tested under a range of 6 different feed temperatures (20ºC; 35ºC; 50ºC; 65ºC; 80ºC and 95ºC), while the cold feed was kept constant at 5ºC. Partial pressure differences were calculated for each set of temperatures using Antoine's equation:

$$P = e^{\left(23.328 - \frac{3841}{T-45}\right)} \quad \textbf{(1)}$$

where the water vapour partial pressure P is in Pa and the temperature T in Kelvin (K).

II. Results

A. Membrane Characterization

Self-supporting BP membranes (Figure2) are a network of randomly orientated CNTs. These self-supporting BPs were thoroughly characterized in a previous study [9] and found to exhibit many properties desirable for DCMD [7]. Most importantly they exhibit a high porosity (~90%) and contact angle with deionised water (~120°), a thermal conductivity of ~2.3 W/m×K and a tensile Young's modulus of ~1 GPa. Both SEM analysis and particle exclusion tests gave an average pore size of ~25 nm, and BET tests indicated a high specific surface area of ~200 m^2/g comparable with other reports in the literature [14].

The "sandwiched BP" composite structures were expected to exhibit similar properties to the self-standing BPs. As shown in Figure 3, the primary effect of the PP support is to reduce the BP surface area exposed to both permeate and feed streams. The process of hot pressing may also slightly compact the BP structure but further characterization work is needed to confirm this. The characterization results are summarized in Tables 1. BET surface area is also much lower for "sandwiched BP". This value is an artifact of the measurement since PP supports exhibit much lower surface area than self-supporting BPs, while being, in weight, the major component of the composite. The specific surface area of the active layer of the membrane is expected to be similar to a self-supporting membrane. In contrast, the polymer infiltrated BP membranes exhibit a lower specific surface area of ~50 m^2/g, as well as a reduced hydrophobicity of ~100°, compared to the pure self-supporting membranes. Figure 4 shows the surface of a representative BP which was infiltrated with a 5% PS solution. The PS seemed to coat partially some nanotubes reducing the membrane specific surface area. The reduced hydrophobicity is likely caused by the higher surface energy of the infiltrated polymer [15], although a reduced surface roughness, due to the slight compression, may also contribute.

Comment [MCD3]: Where is table 1?

Comment [MCD4]: Where is this data?

Comment [MCD5]: Please unify your terms in text with table. Maybe use a systematic code.

Comment [MCD6]: Where is table 1?

Deleted: The characterization results are summarized in Tables 1.

B. Membrane Distillation Results

1) Membrane Permeability

The measured fluxes are plotted in Figure 5 as a function of the water vapour partial pressure difference across the membrane. While self-supporting BP membranes presented fluxes around 6 to 10 $kg/m^2 \times h$ maximum, composite membranes showed fluxes up to 15 $kg/m^2 \times h$, for water partial pressure differences in the range of 5 to 45 kPa. As expected from theory [16] , the flux increases linearly with water vapour partial pressure for every membrane. Permeances were calculated by taking the gradient of a the best linear fit to the curves in Figure 5. Permeabilities were calculated by multiplying permeances by the

Comment [MCD7]: It might be OK here, but in future, I think is a good idea to fix the lines you fitted to pass through 0,0.

average active thickness of the membrane.

The calculated permeabilities were comprised between 1.6 and 3.3 x 10^{-12} kg/(m×s×Pa) for the composite CNT membranes (Table 3). These values are up to four times the permeabilities of self-supporting membranes, clearly demonstrating the potential of composite BP membranes.

"Sandwiched BP" membranes gave the best permeabilities of all the composite BP membranes, with a value of 3.3 x 10^{-12} kg/(m×s×Pa). Although the "filtered sandwich BP" membrane was very similar in structure, its permeability was half that of the "sandwich BP" membrane. This may result from a thicker CNT active layer. The "filtered sandwich BP" membranes were processed by filtering the CNTs through the PP support so that CNTs partially occupied the pores of the PP support while also forming a layer on top of it. Further characterisation work is needed to confirm this. The lower permeabilities measured for the "polymer infiltrated BP" membranes are consistent with the characterisation results indicating a reduced porosity and specific surface area due to the polymer presence.

Even if composite BP membranes show improved performances, those values were still 0.5 to 2.5 times lower than the PTFE permeability (Table 2).

This may be firstly attributed to the BP membrane thermal conductivity, which was ~10 times greater than that of PTFE. This higher thermal conductivity could lead to higher heat transfers between feed and permeate thus reducing temperature gradient and vapour pressure difference across the membrane. Secondly, the pore shape of the PTFE membranes was different from the non-woven structure of the BPs. BP pores are an interconnected network of interstitial gaps between CNTs, while PTFE membrane pores are thin and long due to the stretching of the PTFE films during their processing. Their pores are also likely to be much straighter than the BPs' pores, leading to a less tortuous path. Also, the BP average pore size was ~10 times smaller than for PTFE membranes, and the Theory of Knudsen diffusion predicts that the molar flux should be proportional to the radius of the pores, which would have an important impact on the results [17].

Finally membrane ageing, as discussed in the next section, may also contribute to lowering the performances. But further work is needed to confirm this assumption.

2) Lifespan and salt rejection

The composite BP membranes exhibited improved salt rejection and lifespan compared with self-supported structures. The lifespan was defined as the time taken for the salt rejection to drop below 90%. As shown in Figure 6, a slow increase in permeate conductivity, and hence a reduction in salt

Deleted: to the one measured for the pure
Deleted: ,
Deleted: potential
Deleted: is
Deleted: is
Deleted: of
Deleted: more than likely
Deleted: partially
Deleted: in
Deleted: remain in average
Deleted: is
Deleted: is
Deleted: At last but not least
Deleted: is
Deleted: .
Deleted: on
Deleted: shows
Deleted: .
Deleted: F
Deleted: although

rejection, was observed over time for the most of the tested BP membranes. This was related to membrane ageing as discussed later. The best lifetime of 39 hours was recorded for the “sandwiched BP” composite membranes and is 13 times higher than for self-supporting BP membranes. Most of the membranes maintained high salt rejections for longer than 25 hours of continuous operationfor different tests conditions, whereas all self-supporting membranes cracked after approximately 3 hours of continuous testing. This improvement was likely due to extra reinforcement given by the PP supports and infiltrated polymers.

The average salt rejection was increased from 90% for self-supporting BPs to 95% on average for the composite BP membranes (Table 2). With further optimization of the composite structures it is hoped that 99.99% efficiency will be achieved as observed for control PTFE membranes.

While the composite BP membrane results are encouraging, membrane ageing is still the major factor limiting their performance at this stage. Cross sections of the BP structures were exposed by Focus Ion Beam milling, as shown in Figure 7. Cracks were found propagating in some regions across the membranes. EDS analysis showed the presence of salts in these cracks, confirming that bridges of salty water cross the membrane from the feed to permeate. However, crack formation in composite membranes was slower, because the PP supports or infiltrated polymers reduced cracking. Lifespan was increased and the rate of conductivity rise slowed down substantially when composite rather than self support CNT BPs were used.

The composite BP structures will be further optimised and other embedding methods and structures investigated to further extend membrane lifespan and improve their performance.

Deleted: is

Deleted: is

Deleted: in greater detail below

Deleted: worked

Deleted: in a row

Deleted: and under

Deleted: always

Deleted: in average

Deleted: is

Deleted: in

Deleted: at this stage

Deleted: done

Deleted: on the BP structures

Deleted: to be

Comment [.8]: Should this be EDAX?

Deleted: material

Deleted: seemed to be

Deleted: slowed

Deleted: down by

Deleted: and the amount of salts present was reduced compared to the self-supporting structures.

III. Conclusion

We demonstrated that composite material BP membranes have comparable flux and permeability to PTFE membranes. The lifespan of BP membranes was increased by a factor 10, with membranes lasting for more than 39 hours of continuous operation when reinforcing was used, while the salt rejection efficiency of the composite structures was on average 95%, reaching 98.5% for multi-layer composite structures.

"Sandwiched composite BP" were in this work the most efficient structures and multi-layer composite membranes showed encouraging results and behaviour. However, different geometries or material supports should be considered for optimizing the performances of the membranes.

Further work is required to fully understand their properties and behaviour and to maximise their potential in MD. Work is under way to fully characterize the BP thermal behaviour and identify how their heat diffusivity and heat conductivity affect the flux and temperature gradient. Other composite material membranes will be processed to optimize the performances of CNT BP membranes in DCMD. Membranes based on larger pore size CNTs may lead to improved flux and performance, while stiffer reinforcements or better connectivity between CNTs may further reduce ageing effects. Furthermore, different setups such as Vacuum Membrane Distillation (VMD) may be tested if considered more suitable than DCMD for the BP structure and properties.

Deleted: present

Deleted: with

Deleted: 40

Deleted: in a row

Deleted: in

Deleted: brought up to

Deleted: while

Deleted: to

Deleted: e

Deleted: while taking the best from the CNTs properties

Deleted: However f

Deleted: setup

Deleted: the

Deleted: L

Deleted: based membrane

Deleted: answer the

Deleted: issue

Acknowledgments

The author would like to thank CSIRO Material Science and Engineering and the Institute for Sustainability and Innovation at Victoria University for financial support. We highly appreciated *Dr. Stephen Hawkins* and *Chi Huynh* nanotube quality and thank them for providing us with their high grade material (CSIRO MSE). We gratefully acknowledge Dr. *John Ward* and *Mark Greaves* (CSIRO MSE) for their expert advice on SEM, and Dr. *Sergey Rubanov* and *Kenneth Goldie* (Bio21 – Melbourne University) for focused ion beam milling. Thanks also to *Mark Hickey* and *Robin Cranston* for their help on several technical matters, and to *Chi Huynh* for providing us with high grade CNTs (CSIRO MSE). We would also like to thank *Zongli Xie* (CSIRO MSE) and *Lisa Wong* (CSIRO Petroleum Resources) for their help with BET measurements, Dr. *Julie Nigro* for her advice with the fluorescence tests (CSIRO MHT), Dr. *Shane Cox*, (UNSW – Australia), for his assistance with porometer measurements and finally, Dr. *Jun De-Li* and *Jianhua Zhang* for their assistance with heat conductivity tests (Victoria University).

Deleted: his appreciated

Deleted: Porometer

Comment [MCD9]: It would be good to acknowledge the MSA Millipore Award and the AMS-MSA poster awards.

List of figures :

Figure 1 Direct Contact Membrane Distillation concept.
Figure 2 Representative SEM image of the surface of a self-supporting BP membrane.
Figure 3 Representative SEM image of the structure of the PP support.
Figure 4 Representative SEM image of a the surface of a PS infiltrated composite BP membrane.
Figure 5 Flux as a function of vapour pressure difference (dP) across the membrane. The vapour pressure difference was controlled by varying the hot side temperature (20ºC; 35ºC; 50ºC; 65ºC; 85ºC 95ºC) while maintaining a constant cold side temperature of 5ºC. Feed flow of 300 mL/min. Conductivity hot side ~11 mS.
Figure 6 Variation of permeate conductivity over time for a representative BP composite membrane and a PTFE membrane.
Figure 7 Left: SEM image of a section milled with a Focus Ion Beam through a BP membrane after testing in the DCMD setup. Right: corresponding EDS analysis showing the presence of salts in the crack.

Comment [.10]: EDAX rather than EDS?

List of tables :

Table 1 Properties of BP membranes
Table 2 Salt rejection, permeability and life of tested membranes

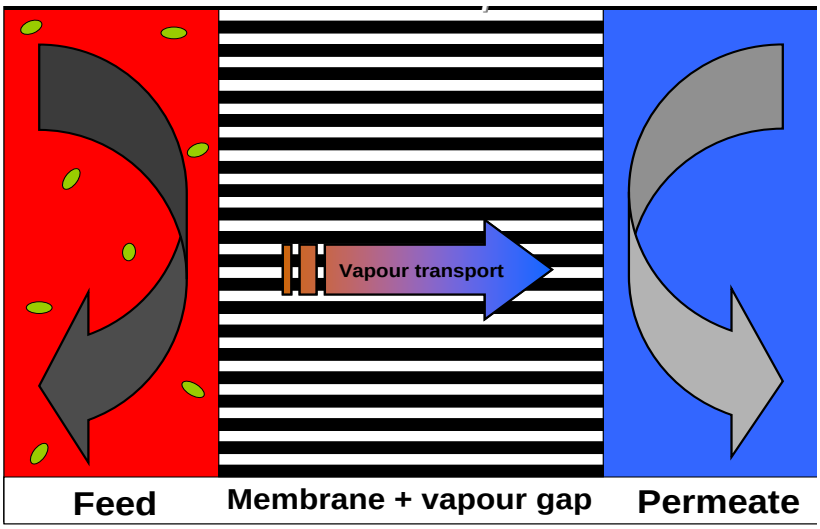

Figure 1 Direct Contact Membrane Distillation concept.

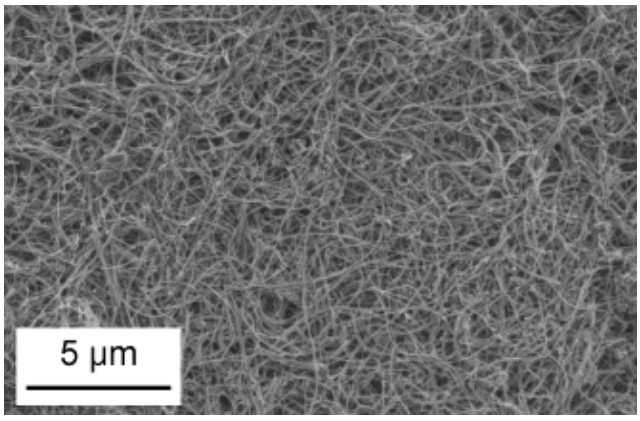

Figure 2 Representative SEM image of the surface of a self-supporting BP membrane.

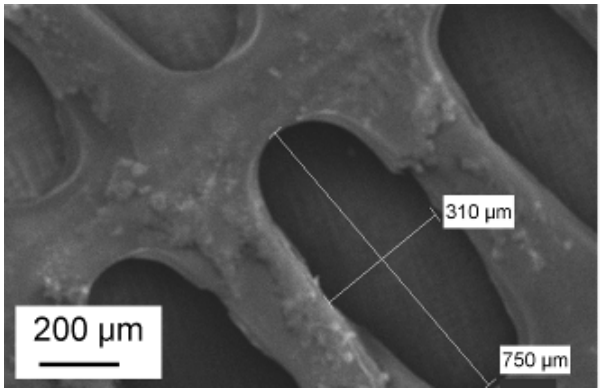

Figure 3 Representative SEM image of the structure of the PP support.

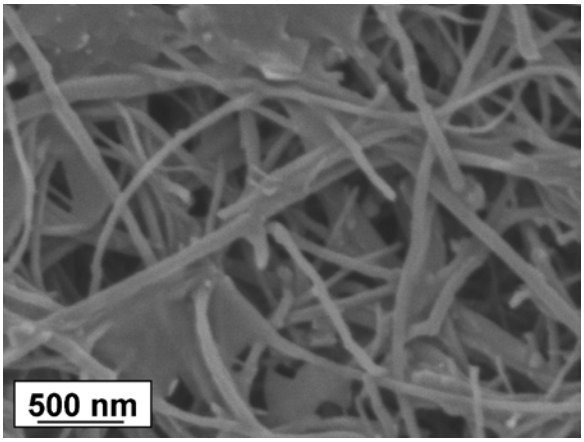

Figure 4 Representative SEM image of at the surface of a PS infiltrated composite BP membrane.

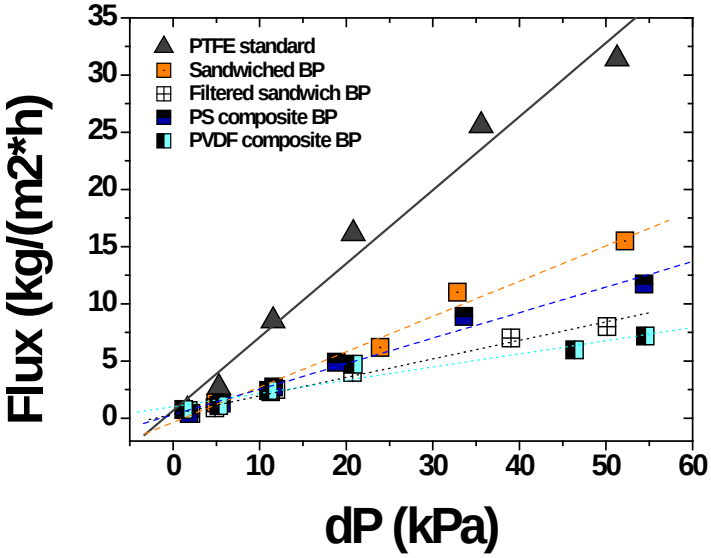

Figure 5 Flux as a function of vapour pressure difference (dP) across the membrane. The vapour pressure difference was controlled by varying the hot side temperature (20°C; 35°C; 50°C; 65°C; 85°C 95°C) while maintaining a constant cold side temperature of 5°C. F

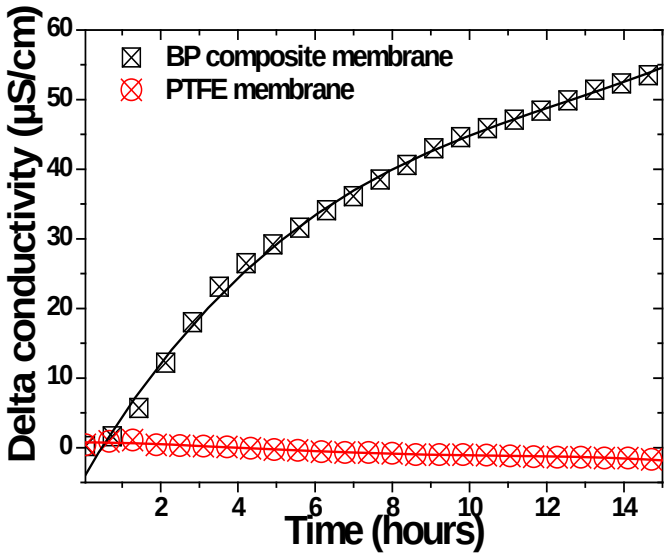

Figure 6 Variation of permeate conductivity over time for a representative BP composite membrane and a PTFE membrane.

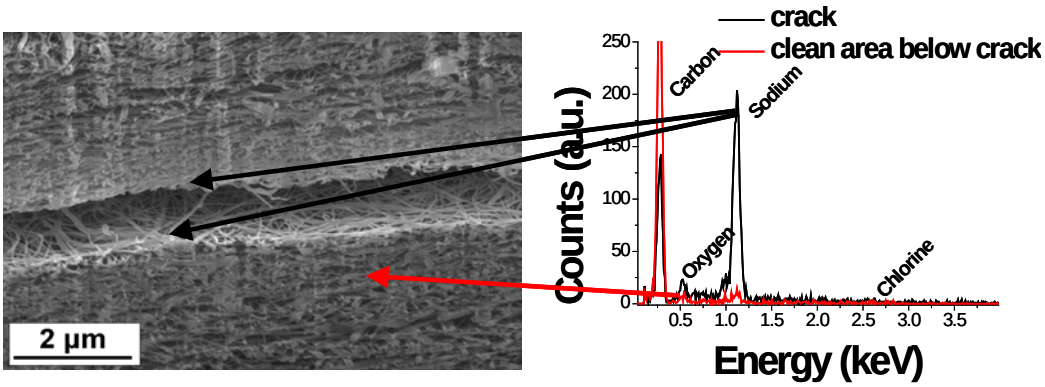

Figure 7 Left: SEM image of a section milled with a Focus Ion Beam through a BP membrane after testing in the DCMD setup. Right: corresponding EDS analysis showing the presence of salts in the crack.

Table 1 Properties of BP membranes

	Contact angle	*Porosity*	*Pore size SEM imaging*	*Bubble point*	*LEP water*	*BET*	*Thermal conductivity*
	°	*%*	*nm*	*PSI*	*PSI*	*m^2/g*	*$W/m^2 \times K$*
PTFE 0.2µm pores	**130**	**70-75**	**200-400**	**14.5**	**50**	**21**	**0.25**
Self-supporting BP	**115-125**	**85-90**	**25-100**	**5.5**	**8**	**197**	**2.3**
Composite multi layer	**90-100**	**~75**	**25-100**	**-**	**-**	**21***	**-**
Polymer infiltrated composite	**95-110**	**~60**	**25-100**	**-**	**-**	**50**	**-**

* Mass of sample included the PP support in the calculation

Table 2 Salt rejection, permeability and life of tested membranes

	Thickness	*Salt Rejection**	*Lifespan***	*Permeability*
	µm	*%*	*hours*	*10^{-12} kg/(m*s*Pa)*
PTFE 0.2µm pores	**~200**	**99.9**	**-**	**5.51**
Self-supporting BP	**from 20**	**~ 90**	**3**	**0.83**
Composite multi layer	**~120-140**	**95.5**	**39**	**3.31**
Filtrated BP through support	**~120-140**	**94.7**	**34**	**1.55*****
Polymer infiltrated PS	**~40-80**	**98.5**	**19**	**2.57**
Polymer infiltrated PVDF	**~40-80**	**96.5**	**16**	**1.89**
Poly-propylene support	**~100**	**-**	**-**	**-**

* For intact membranes

** Calculated for 90% salt rejection

*** Thickness of active layer considered: 40 µm

Deleted: ^

References

[1] Iijima, S., *Helical microtubules of graphitic carbon.* Nature, 1991. **354**(6348): p. 56-58.

[2] Peng, F., C. Hu, and Z. Jiang, *Novel ploy(vinyl alcohol)/carbon nanotube hybrid membranes for pervaporation separation of benzene/cyclohexane mixtures.* Journal of Membrane Science, 2007. **297**(1-2): p. 236-242.

[3] Fornasiero, F., H.G. Park, J.K. Holt, M. Stadermann, C.P. Grigoropoulos, A. Noy, and O. Bakajin, *Ion exclusion by sub-2-nm carbon nanotube pores.* Proceedings of the National Academy of Sciences of the United States of America, 2008. **105**(45): p. 17250-17255.

[4] Hinds, B.J., N. Chopra, T. Rantell, R. Andrews, V. Gavalas, and L.G. Bachas, *Aligned multiwalled carbon nanotube membranes.* Science, 2004. **303**(5654): p. 62-65.

[5] Srivastava, A., O.N. Srivastava, S. Talapatra, R. Vajtai, and P.M. Ajayan, *Carbon nanotube filters.* Nat Mater, 2004. **3**(9): p. 610-614.

[6] Lawson, K.W. and D.R. Lloyd, *Membrane distillation. II. Direct contact MD.* Journal of Membrane Science, 1996. **120**(1): p. 123-133.

[7] Schofield, R.W., A.G. Fane, C.J.D. Fell, and R. Macoun, *Factors Affecting Flux in Membrane Distillation.* Desalination, 1990. **77**(1-3): p. 279-294.

[8] Gryta, M., M. Tomaszewska, and K. Karakulski, *Wastewater treatment by membrane distillation.* Desalination, 2006. **198**(1-3): p. 67-73.

[9] Dumée, L., K. Sears, J. Schütz, N. Finn, M. Duke, and S. Gray, *Characterization and evaluation of carbon nanotube bucky-paper membranes for direct contact membrane distillation.* Journal of Membrane Science, Submitted July 2009.

[10] Huynh, C. and S. Hawkins, *Understanding the synthesis of directly spinnable carbon nanotube forests.* Submitted to Carbon, 2009.

[11] Smolders, K. and A.C.M. Franken, *Terminology for Membrane Distillation.* Desalination, 1989. **72**(3): p. 249-262.

[12] Cooper, S.M., H.F. Chuang, M. Cinke, B.A. Cruden, and M. Meyyappan, *Gas Permeability of a Buckypaper Membrane.* Nano Letters, 2003. **3**(2): p. 189-192.

[13] Nuriel, S., L. Liu, A.H. Barber, and H.D. Wagner, *Direct measurement of multiwall nanotube surface tension.* Chemical Physics Letters, 2005. **404**(4-6): p. 263-266.

[14] Smajda, R., A. Kukovecz, Z. Konya, and I. Kiricsi, *Structure and gas permeability of multi-wall carbon nanotube buckypapers.* Carbon, 2007. **45**(6): p. 1176-1184.

[15] Instruments, D.P. *Solid surface energy data (SFE) for common polymers.* 2007; Available from: http://www.surface-tension.de/solid-surface-energy.htm.

[16] El-Bourawi, M.S., Z. Ding, R. Ma, and M. Khayet, *A framework for better understanding membrane distillation separation process.* Journal of Membrane Science, 2006. **285**(1-2): p. 4-29.

[17] Burgoyne, A. and M.M. Vahdati, *Direct Contact Membrane Distillation.* Separation Science and Technology, 2000. **35**(8): p. 1257 - 1284.

LAST PAGE

Deleted: on the 25th of

Deleted: - being reviewed